# Effect of Solution Composition on the Energy Production by Capacitive Mixing in Membrane-Electrode Assembly

Silvia Ahualli,*,[†] M. Mar Fernández,[†] Guillermo Iglesias,[†] María L. Jiménez,[†] Fei Liu,[‡] Martijn Wagterveld,[‡] and Ángel V. Delgado[†]

[†]Department of Applied Physics, School of Science, University of Granada, 18071 Granada, Spain
[‡]WETSUS, Centre of Excellence for Sustainable Water Technology, 8900 CC, Leeuwarden, The Netherlands

ABSTRACT: In this work, we consider the extent to which the presence of multivalent ions in solution modifies the equilibrium and dynamics of the energy production in a capacitive cell built with ion-exchange membranes in contact with high surface area electrodes. The cell potential in open circuit (OCV) is controlled by the difference between both membrane potentials, simulated as constant volume charge regions. A theoretical model is elaborated for steady state OCV, first in the case of monovalent solutions, as a reference. This is compared to the results in multi-ionic systems, containing divalent cations in concentrations similar to those in real seawater. It is found that the OCV is reduced by about 25% (as compared to the results in pure NaCl solutions) due to the presence of the divalent ions, even in low concentrations. Interestingly, this can be related to the "uphill" transport of such ions against their concentration gradients. On the contrary, their effect on the dynamics of the cell potential is negligible in the case of highly charged membranes. The comparison between model predictions and experimental results shows a very satisfactory agreement, and gives clues for the practical application of these recently introduced energy production methods.
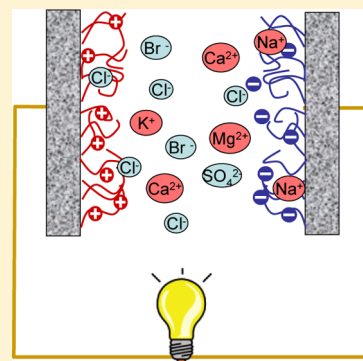
INTRODUCTION

A number of recent papers have shown that energy can be harvested from the unavoidable entropy increase associated with the mixing of solutions with different ionic concentrations.[1] In fact, the methods that can be implemented with that purpose have been jointly denominated as Capmix techniques (www.capmix.eu), and they are intended to produce electrical energy without the intervention of electromechanical devices. Apart from minor variations, the methods can be classified into two groups: one, known as CDLE (or capacitive energy extraction based on Double Layer Expansion) is based on the fundamental fact that electrical double layers increase their thickness when the ionic concentration of the solution in contact with the interface is decreased. This brings about a reduction in capacitance and hence a raise in electric potential at constant charge. The idea was set forward by Brogioli,[2] and much work has been devoted both to its theoretical fundamentation[2-5] and experimental implementation.[6,7]

An alternative technology, using features of both CDLE and reverse electrodialysis (RED)[8-10] has been proposed with the advantage of not requiring redox solutions as in RED or external charging elements as in CDLE. The technique, known as CDP (or capacitive energy extraction based on Donnan Potential), was first elaborated by Sales et al.[11] As shown in Figure 1, water solutions are pumped through a channel limited by anion and cation exchange membranes, respectively, in close contact with activated carbon films deposited on a (typically graphite) current collector. Let us assume that initially the whole cell is bathed in the fresh water solution, with short-circuited terminals (Figure 1a). If any cell potential is generated because of small concentration differences between both sides of any of the membranes, then this would be compensated for by electrode charge. If now seawater is allowed in the spacer (Figure 1b) under open circuit conditions, then a membrane potential will be generated (negative at the anionic side and positive at the cationic one), and a potential difference will be measured. If a load is connected to the cell, then current will flow externally until the electric potentials at both electrodes are equal (Figure 1c), and hence electric energy is extracted during this stage. The potential difference between the electrodes will be zero, but charge has been transferred from one to the other, both being charged in consequence. The circuit is open and fresh water is pumped again, with the result that the membrane potential goes to zero again and the electrodes gain potential due to the transferred charge obtained in the previous step (Figure 1d). If the external load is connected, then current flows in the opposite direction and work is extracted again. In a modification of the technique, the "natural" charging and discharging processes just described are externally forced by means of a current source, and more energy can be obtained.[12] Additionally wire-shaped electrodes have been proposed as a convenient alternative to the standard flat membrane approach.[13] (The actual cell used for the experiments described in this paper is shown in Figure 1e.)
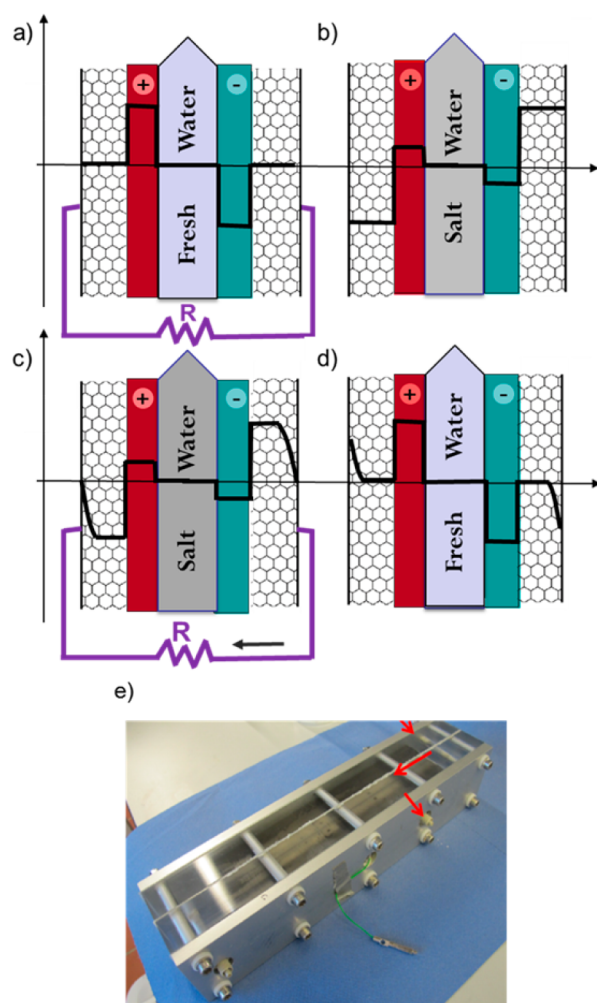
Figure 1. Schematics of the CDP methodology. Electrostatic potential profile when (a) fresh water flows through the spacer between anion and cation exchange membranes, with short-circuited electrodes; (b) salt water flows under open circuit conditions; (c) the electrodes are connected by means of a load resistance, and the electrode potential decreases as charging proceeds; (d) fresh water is pumped in open circuit, leaving the cell ready for stage (a) again. (e) Picture of the cell: the arrows indicate the path of the pumped solutions. The membranes and the spacer are sandwiched between two plastic pieces.

Previous models on the phenomena have considered that the exchanging solutions are simply NaCl of specified concentrations (500−600 mM and 20 mM),[11,12] and are based on simple assumptions for membrane processes responsible for the phenomenon. However, both the results obtained with the simpler CDLE technique[14] and many studies involving the physical chemistry of membranes[15,16] show that the presence of complex solutions containing ions of different valencies and diffusion coefficients can introduce very important differences with respect to results found with simple solutions. This suggests that an exhaustive characterization of the method with real sea and river waters is mandatory prior to the upscaling for practical applications. Experiments in this field have focused on the scaling and biofouling of membranes, which is a difficult task, but a classical problem in membrane applications. Nevertheless, even a clean sample of sea or river water, with no particulates, and free from fouling problems, is made of ionic species other than Na$^+$ and Cl$^-$, with different charges, sizes, and diffusion rates. However, as far we know, the extent to which such complicating factors affect the energy production of a CDP device is still unknown. In particular, the process of ionic diffusion inside membranes includes uphill transport of ions in multi-ionic solutions, as recently shown with the reverse electrodialysis technique.[17] Hence, a suitable approach to the understanding of CDP kinetics must include an analysis of the dynamics inside the membranes.

In the present work, we focus on the theoretical model of the dynamics inside a membrane in which both sea and river waters are composed by multi-ionic solutions. We also apply this model to the energy production with the CDP technique and compare it with experimental results.

◼ GENERAL ASPECTS OF THE EQUILIBRIUM MEMBRANE MODEL

Simple Ionic Solutions. In the cycle described in Figure 1 there are four stages, two of them in open circuit, and two in closed circuit. In the former case, the dynamics of the Donnan potential establishment in the membranes is controlled by the membranes themselves, while in the second case, a current will flow through the membrane and in the external circuit. Both stages require two different approaches, and hence, we will study them separately.

We start by considering the simplest model of an ion exchange membrane[18,19] which we can think of. It will be a region where a given amount of volume charge (coming from the dissociation of fixed molecular groups) is distributed. When a positively charged membrane is placed in contact with an electrolyte solution, mainly anions will be able to get inside the membrane, while cations can preferably penetrate a negatively charged one (Figure 2). They are respectively denominated anionic and cationic membranes. In both cases, they will be characterized by their thickness, water content, swelling behavior, and permselectivity. Our target is the calculation of the membrane potential (potential difference between opposite faces) for given differences between the electrolyte concentrations on both sides. The membrane is planar, hence, we
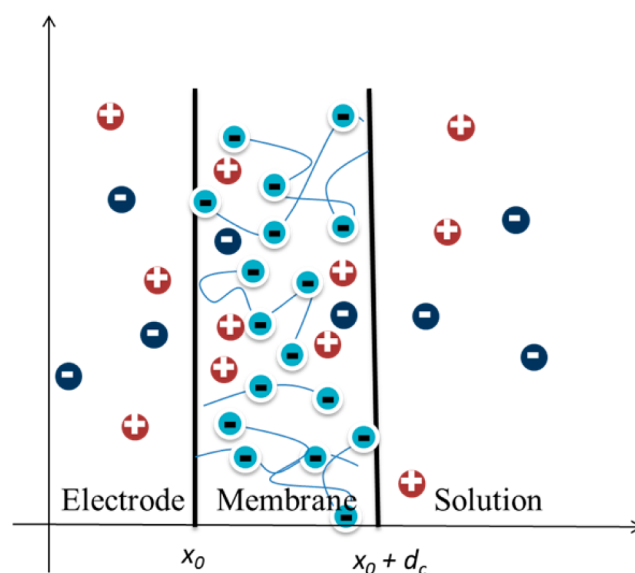
Figure 2. Simplified scheme of a cationic membrane. Fixed charges of the polymer chain (negative in this case) are depicted in light blue, while free ions are represented in dark blue and red. x_0 is the position of the left wall of the membrane and d_c its thickness.
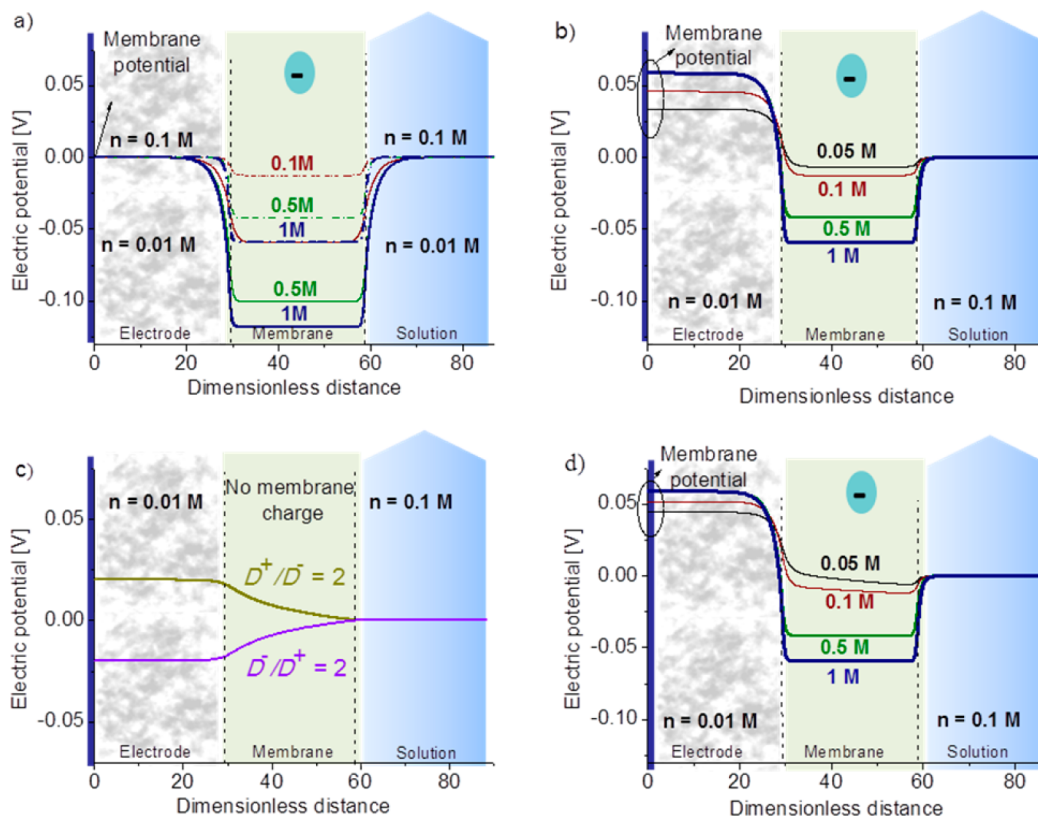
Figure 3. Electric potential profiles in and around a membrane delimited by the dotted vertical lines for (a) the same concentration baths in both sides of the membrane (dashed lines: 0.1 M; solid lines: 0.01 M), and (b) different ionic concentrations on each side (left side, 0.01 M and right side 0.1 M). The charge of the membrane is indicated in units of mol/L, and ranges from 0.05 M (4.8×10^6 C/m^3) to 1 M (9.6×10^7 C/m^3). The ionic diffusion coefficient for both monovalent ionic species is 2×10^{-9} m^{2}s^{-1}. (c) Same as case (b) but the membrane is uncharged, and the ratio between diffusion coefficients is as indicated. (d) Same as Figure (b) but for the case D$^+$/D$^-$ = 2.

consider homogeneous the properties at every plane parallel to the membrane surface. This simplifies the problem to a one-dimensional one, that is, only variations of the quantities of interest in the perpendicular direction (x hereafter) are considered.

We assume that the membrane contains a homogeneous volume charge density, ρ_{memb}. We denote by n_i the concentration of ions of type i at any position, and by z_i their corresponding valencies. Outside the membrane, in the solution volume, the relative permittivity is ε, and inside it, its value is ε_m. The Poisson equation, governing the electric potential Ψ will read, in each region:

$$\begin{cases} \dfrac{d^2\Psi}{dx^2} = -\dfrac{1}{\varepsilon\varepsilon_0}\sum_{i=1}^{N} z_i e n_i \\ \qquad \rightarrow \text{ outside the membrane} \\[6pt] \dfrac{d^2\Psi}{dx^2} = -\dfrac{1}{\varepsilon_m\varepsilon_0}\sum_{i=1}^{N} z_i e n_i - \dfrac{\rho_{memb}}{\varepsilon_m\varepsilon_0} \\ \qquad \rightarrow \text{ inside the membrane} \end{cases} \quad (1)$$

These equations are completed by assuming steady state conditions, and, according to the Nernst−Planck conservation equation for each ionic species, specifying that the flux is uniform inside the membrane:

$$J_i = \text{constant} = C_i \quad i = 1, ..., N \quad \text{inside the core} \quad (2)$$

where the ionic flux consists of diffusive and electromigration contributions:

$$J_i = -D_i\frac{dn_i}{dx} - D_i\frac{e}{kT}z_i n_i\frac{d\Psi}{dx} \quad (3)$$

Here, D_i is the diffusion coefficient, k the Boltzmann constant, and T the absolute temperature.

Note that our treatment does not need to assume a value for the potential jump outside the membrane. Instead, a potential distribution on both sides of the membrane is predicted as a natural consequence of the consideration that the ion flux is constant.

Summarizing, the equations governing the ionic concentrations (and, with eq 1 the potential) are as follows:

$$\begin{cases} \dfrac{dn_i}{dx} = -\dfrac{e}{kT}z_i n_i\,\dfrac{d\Psi}{dx} \quad i = 1, ..., N \quad \text{outside the membrane} \\[10pt] D_i\dfrac{dn_i}{dx} = C_i - \dfrac{e}{kT}z_i n_i D_i\dfrac{d\Psi}{dx} \quad i = 1, ..., N \quad \text{inside the membrane} \end{cases} \quad (4)$$

For solving this system, the following boundary conditions are required, regarding the continuity of the potential, of the electric displacement and of the ionic concentrations at the

electrode-membrane ($x = x_0$) and membrane-solution ($x = x_0 + d_c$) interfaces:

$$\psi|_{x_0^-} = \psi|_{x_0^+}$$

$$\psi|_{(x_0+d_c)^-} = \psi|_{(x_0+d_c)^+}$$

$$\varepsilon \frac{d\psi}{dx}\bigg|_{x_0^-} = \varepsilon_m \frac{d\psi}{dx}\bigg|_{x_0^+}$$

$$\varepsilon \frac{d\psi}{dx}\bigg|_{(x_0+d_c)^-} = \varepsilon_m \frac{d\psi}{dx}\bigg|_{(x_0+d_c)^+}$$

$$n_i|_{x_0^-} = n_i|_{x_0^+} \quad i = 1, ..., N$$

$$n_i|_{(x_0+d_c)^-} = n_i|_{(x_0+d_c)^+} \quad i = 1, ..., N \tag{5}$$

At large distances from the membrane-solution boundaries:

$$\psi|_{x \to -\infty} = E_m$$

$$\psi|_{x \to \infty} = 0$$

$$n_i|_{x \to -\infty} = n_{i,I} \quad i = 1, ..., N$$

$$n_i|_{x \to \infty} = n_{i,II} \quad i = 1, ..., N \tag{6}$$

where E_m is the membrane potential; this is one of the unknowns of the problem, together with the profiles of electric potential $\psi(x)$, the electric field $d\psi(x)/dx$ and ion concentrations, n_i. $n_{i,I}$ and $n_{i,II}$ are the concentrations of the solution reservoirs in the left and right sides of the membrane, respectively. Such concentrations are always constant, that is, the volume of both reservoirs is very large in comparison with that of the membrane. Summarizing, the unknowns are $\psi(x)$, $d\psi(x)/dx$, n_i in each of the three regions, that is, $3(N + 2)$ for the whole problem. It is worth to mention that E_m and C_i also are unknowns, hence the number of boundary conditions must be $3(N + 2)$ plus $(1+N)$. From eqs 5,6 we have $4N + 6$. Hence we need an additional condition: this regards the ion fluxes (eq 2), and the specification that in equilibrium the current must vanish:

$$\sum_{i=1}^{N} z_i e J_i = 0 \tag{7}$$

Depending on the relationship between the membrane thickness and that of the electric double layer (or Debye length, $1/\kappa$), a uniform potential will be reached in the membrane, far from its limiting walls (Figure 3a). This is the Donnan potential, controlled by the ionic concentration of the solution bathing the membrane: note how it decreases if the solution in contact is concentrated. If, instead, the concentrations in both sides of the membrane are different, then it is precisely the difference between the Donnan potentials on each side that provokes the appearance of a so-called membrane potential, as indicated in Figure 3b. Note that in this and subsequent figures, distances are made dimensionless by using the factor $(n_{ref}e^2/\varepsilon_0\varepsilon_m kT)^{1/2}$, where n_{ref} is the highest electrolyte concentration in contact with the membrane.

In addition to the generation of the Donnan potential, another phenomenon of interest for our purposes takes place in the membrane interior, namely, the establishment of a diffusion potential, related to the concentration differences of ionic species diffusing at different velocities (for instance, in mixed solutions). This can be observed in Figure 3c, where a zero

membrane charge is assumed with the aim of making clear the effect of the diffusion potential on the membrane potential. Note that the fastest ion is determinant of the potential.

The profile of potential is plotted in Figure 3d for different membrane charges and combinations of diffusion coefficients. As observed, when the membrane charge is small (-0.05 M) the membrane potential is controlled by the gradient of diffusion potential. In contrast, if the charge is high (-1 M in Figure 3d), it is the difference in Donnan potentials that determines the membrane potential. This is not only important from the point of view of the physics of the membrane, since, as we will notice below, the energy available from the CDP process (the membrane/carbon electrode combination) is also dependent on these two contributions. In practice, highly charged membranes will be preferred for CDP operation, although this characteristic is not always guaranteed, as (bio)fouling of the membrane might reduce the effective charge of an originally highly charged membrane. Hence, the importance of modeling in this respect, mainly if, as it will be the case, we may have as many as 7 different ionic species in solution.

The Case of Multi-Ionic Solutions. We are now in position of comparing the membrane potentials attained in solutions composed of just two ionic species (monovalent, as typically used in the Capmix tests) to those in mixed solutions with arbitrary concentrations of whatever ions. In this new step, the solution simulating the high concentration bath (the sea) is composed of the salts detailed in Table 1,[20,21] whereas the river

Table 1. Ionic Composition of Standard (Artificial) Sea Water

salt	concentration (g/L)	concentration (mol/L)
NaCl	23.375	0.400
MgSO$_4$	2.405	0.020
CaCl$_2$	1.11	0.010
MgCl$_2$	1.904	0.020
KCl	0.745	0.010
KBr	0.203	0.0017

water is assumed to contain the same salts with concentrations reduced by a 1/30 factor. Note that, in spite of the relatively high ionic strengths of these solutions, concentrations (and not activities) can be safely used for all calculations, as the membrane potential will be roughly controlled by the logarithm of the activity ratio, and the effect of the activity coefficient ratio will cancel out in comparison with that of the concentration ratio ($\ln[1/30]$).[22]

Figure 4 shows the potential profiles and hence the membrane potentials reached (with respect to a reference on the right of the membrane, far from the interface) in two cases: in the presence of 511.7 mM and 511.7/30 mM NaCl on each side of the membrane, and in the presence of the same concentrations, obtained as the mixtures referred to above.

As observed, the membrane potentials decrease from 83.3 mV in the case of the standard NaCl solution to 54.7 mV in the multi-ionic system. In addition, the different diffusion coefficients of cations and anions makes it very difficult to obtain a symmetric behavior in the cationic and anionic membranes (compare the solid and dashed lines in the Figure). The differences are more accentuated in the case of the multi-ionic solutions, where positive and negative ions contribute to increase the lack of symmetry mentioned, if we assume that
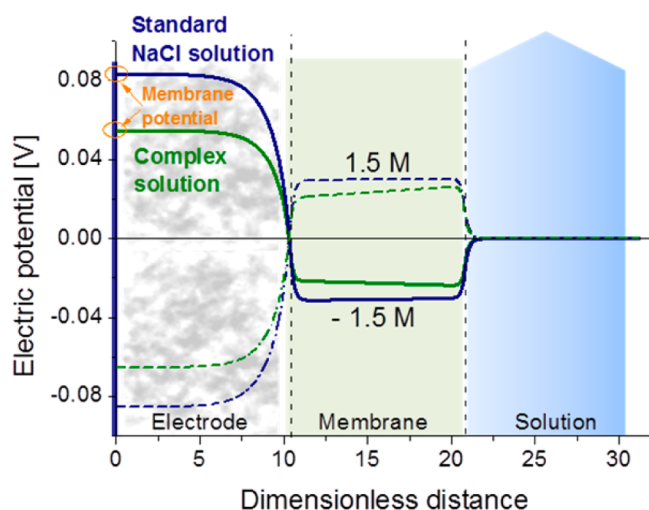
Figure 4. Comparison of the electric potential profiles for a complex solution with the concentrations indicated in Table 1, and the corresponding standard NaCl solution in such a way that the concentration of positive and negative species are in both cases 511.7 mM at the right side of the membrane and a fraction 1/30 at the left. The charge of the membrane is −1.5 M (solid lines) and +1.5 M (dashed lines).

both the anionic and cationic membranes contain comparable amounts of charged groups except for the obvious difference in their sign.

It is interesting at this point to analyze the basis for the reduced membrane potential attained in the case of complex solutions. In reality, this is just for the sake of information, as it is clearly impractical to treat the seawater for eliminating the "undesired" ions (if any) before entering the Capmix cell. Nevertheless, these criteria can help in finding the correct location, in terms of the ionic contents of the seawater.

Our approach consists of isolating the roles of the different kinds of counterions (cations in the case considered; the calculations can be easily reformulated for the oppositely charged membrane of the cell). With that aim, we have calculated the membrane potential assuming that the co-ions in Table 1 are at the concentrations indicated in the Table, but only one counterion is used each time (that is, 511.7 mM Na^+, or 255.85 mM Ca^{2+}, for instance; a similar study was carried out with co-ions, but, as expected, their role is not significant in this respect). Table 2 summarizes the results.

Table 2. Theoretical Membrane Potential

counterion/concentration [mM]	diffusion coefficient [m^2/s]	membrane potential [mV]
Na^+/ 511.7	1.35×10^{-9}	83.6
Mg^{2+}/ 255.85	0.706×10^{-9}	38
K^+/ 511.7	1.96×10^{-9}	84.7
Ca^{2+}/ 255.85	$0.792 \times 10{-9}$	38.6

Data for a membrane charged with 1.5 M negative groups, when only the counterions indicated are in solution together the same co-ions indicated in Table 1, keeping constant their concentrations: $[Cl^-]$ = 470 mM, $[SO_4^{2-}]$ = 20 mM and $[Br^-]$ = 1.7 mM. The potential in the multi-ionic solution is 54.7 mV.

It is clearly observed that, for a highly charged membrane as in our case, there is no significant effect of differences in diffusion coefficient, whereas the valency becomes dominant.

The obvious reason is that half the counterions suffice for producing electroneutrality, and this explains the smaller membrane potential.

It only remains to evaluate the role of the different components on the overall decrease in membrane potential, as compared to that in single salt solutions. The results in Table 3 show our predictions for the membrane potential in solutions

Table 3. Theoretical Membrane Potential[a]

| counterion	counterion concentration [mM]	membrane potential [mV]
Na^+	400	84.9
Mg^{2+}	40	43.2
K^+	11.7	87.3
Ca^{2+}	10	43.6

[a]Theoretical membrane potential for the same kind of membrane as in Table 2, assuming again solutions containing a single type of counterion, as indicated, but for the concentrations in Table 1. Co-ions as in Table 2, with concentrations adjusted proportionally as required by electroneutrality. The potential in the multi-ionic solution is 54.7 mV.

containing a single kind of counterions, with the concentration indicated in Table 1, keeping the 1/30 ratio between sea and fresh water, and maintaining the co-ions in the relative concentrations of the Table, recalculated for ensuring electroneutrality. Note how it is the divalent counterions that produce the fall in membrane potential, even if their concentration is relatively low. These conclusions are well confirmed in a series of experiments whose results will be discussed later.

A careful view of the ion concentration profiles inside the membrane when mixed solutions are in contact with it, can help in clarifying the effect of the highly charged ions (Figure 5). Note that both Ca^{2+} and Mg^{2+} appear to be transported "uphill", that is against their concentration gradients. This phenomenon has been described in many studies of transport of mixed solutions through membranes:[15,16] depending on the concentration and mobility of the counterions involved, it is possible that, under conditions of zero electric current in the membrane, the flux of one type of counterions (the slowest cations in our case) will take place in the opposite direction to that of the dominant cations, under the action of the electric field set up by these when diffusing in the direction of their concentration gradient.

■ DYNAMICS OF THE MEMBRANE PROCESS IN OPEN CIRCUIT

Characteristic Times. The dynamics of the CDP process will be controlled by the time required for the establishment of the membrane potential. First the Donnan potential is reached within the time required for the formation of an EDL, typically in the range of μs (see, e.g., ref 23). The contribution of the diffusion potential, although small in the case of highly charged membranes, is slower and can be at the end responsible for the overall dynamics.[24−26] If this is the case, then the time evolution of the membrane potential will be clearly different for KCl and NaCl, since diffusion potential will be absent in the first case, as the diffusion coefficients of K^+ and Cl^- are practically identical, contrary to those of Na^+ and Cl^-. We performed experiments on the time evolution of the membrane potential using solutions of NaCl and KCl, and the results are shown in Figure 6. Note the close similarity of the potential−time relations in both cases, with a rapid increment during the
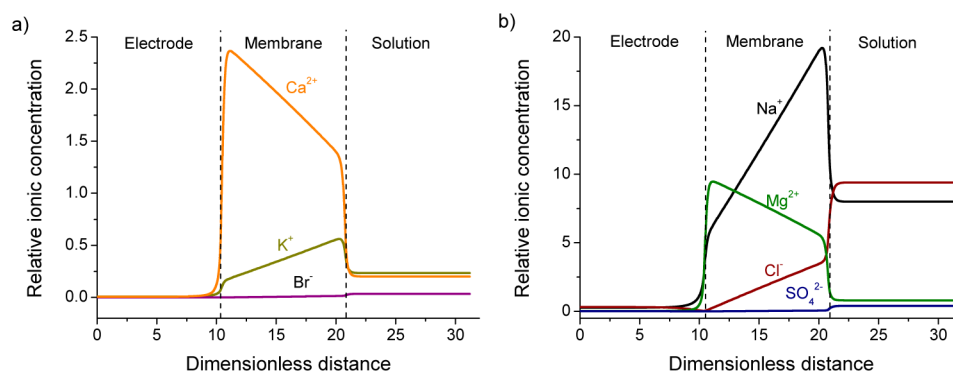
Figure 5. Concentration profiles for the different ions (Table 1) in the conditions given in Figure 4. (a) Ca^{2-}, K^- and Br^- (b) Na^+, Mg^{2-}, Cl^-, and SO_4^{2-}. The ordinate scales are different, so that the profiles for the less abundant ions are appreciable (panel a).
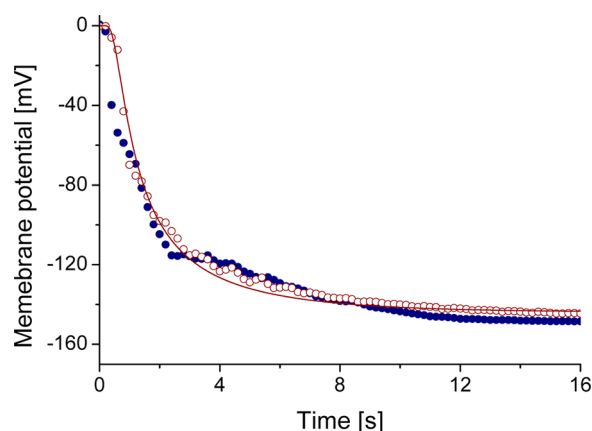
Figure 6. Time evolution of the membrane potential during the exchange from river to seawater in open circuit, in NaCl (open symbols) and KCl (closed symbols) solutions. The maximum potentials reached are, respectively, −144.5 and −148.5 mV. The solid line corresponds to the model predictions for NaCl.

first few seconds, and a slower trend for longer times. In any case, the characteristic time is several orders of magnitude larger than that required for the Donnan potential establishment. These results suggest that the behavior of the membrane with time must be related to the kinetics of the solution in the spacer, controlled by the formation of a convective diffusion layer, as described below.

Convective Diffusion Layer. In the first step of the cycle, the solutions are exchanged by pumping the new solution at a certain velocity. Hence, the membrane will not respond generating the membrane potential instantaneously due to the phenomena associated with the hydrodynamics inside the spacer. Considering diffusive and convective contribution, the ion concentrations follow the Nernst−Planck equation:[27]

$$\mathbf{J}_i = -D_i \nabla n_i + n_i \mathbf{v} \quad i = 1, ..., N \tag{8}$$

where $\mathbf{v}$ is the fluid velocity. Considering first steady state conditions ($\nabla \cdot \mathbf{J}_i = 0$) and using dimensionless variables, we obtain the following:

$$\mathbf{V} \cdot \tilde{\nabla} N_i = \frac{1}{Pe}(\tilde{\nabla}^2 N_i) \tag{9}$$

where $\mathbf{V} = \mathbf{v}/v_0$, $N_i = n_i n_{ref}$), $\tilde{\nabla} = h\nabla$, and Pe is the Peclet number, given by Pe $= v_0 h/D$, v_0 being a characteristic fluid velocity far from the surface, h a characteristic length along which the major concentration changes take place, and D a typical value for D_i. Note that when Pe $\gg 1$, the concentration distribution is largely determined by convective transfer. This is the expected situation in liquids: Pe $=$ Re $\times$ Pr $=$ Re(ν/D), where Pr is the Prandtl number, and ν is the kinematic viscosity. Even in situations of low Reynolds number (Re), Pe is expected to reach high values, ensuring a predominant role of convection over diffusion in the transport of matter in a fluid. However, even for fluid flows with small viscosity, a thin viscous layer has to be taken into account in the vicinity of interfaces.
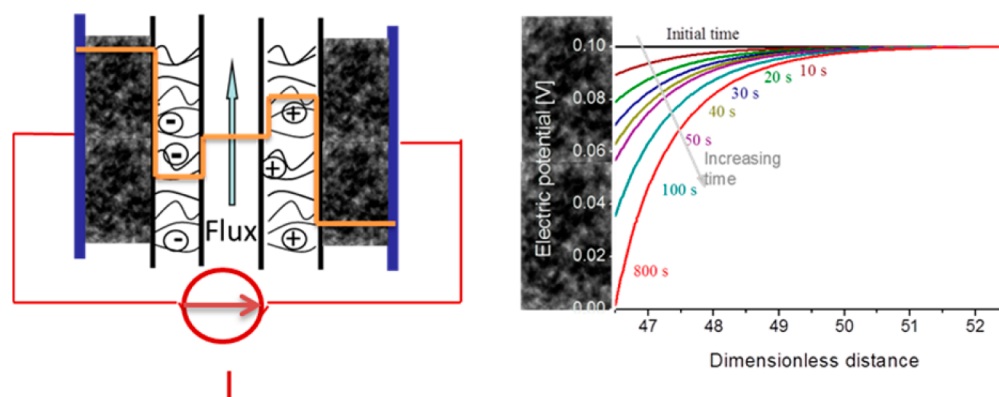
Figure 7. Schematics of the CDP procedure and time evolution of the electrode potential, assuming that a constant current $I = 50$ mA is made to flow through the external circuit. The membrane potential is 100 mV.

Table 4. Experimental Values of Cell Potential and Power Density[a]

NaCl	MgSO$_4$	MgCl$_2$	KCl	KBr	CaCl$_2$	cell potential [mV]	power density [mW/m^2]
400	20	20	10	1.7	10	130	0.340
400	0	0	95.4	16.2	0	145	0.407
400	111	0	0	0	0	122	0.303
511.7	0	0	0	0	0	144	0.400
0	0	0	511.7	0	0	148	0.422

[a]Experimental values of cell potential and the power density achieved in the CDP process for the seawater concentrations indicated in mM (corresponding fresh water composition: 1/30th of the given values). The ionic strength is always the same (511.7 mM) and the first row corresponds to the artificial seawater.

Such a layer, where diffusion cannot be neglected, is known as diffusion boundary layer.[27]

Hence, it is necessary to look into the flow inside the spacer. When the exchange of solutions takes place, the fluid is pumped into the cell at 50 mL/min which according to dimensions of the cell gives a velocity equal to 0.21 m/s. The fluid flows through the cell between two squared electrodes with side 2 cm and separation 200 μm (Figure 1e). A noncircular duct is said to have a hydraulic radius, defined as the ratio between the area of the duct and the wetted perimeter. For our case, the hydraulic radius, 99 μm, allows to predict a Reynolds number of approximately 20, indicating that the fluid behaves as viscous inside the spacer. The problem of the flow between parallel plates has exact analytic solution, yielding a parabolic profile. Then it is possible to consider the diffusion length to be of the same order as half the separation between plates, because the channel is so narrow that there is no space for developing a constant velocity profile.

For estimating the rate of potential increase, we consider that, close to the membrane, diffusion takes place and numerically calculate the ionic concentration at the solution/membrane interface using eq 9 without convection and with planar geometry:

$$\frac{dn_i}{dt} = D_i \frac{d^2 n_i}{dx^2}$$

(10)

From the knowledge of n_i for each time on the membrane solution interface, the membrane potential can be calculated as described in the previous section. The potential predicted as a function of time is represented in Figure 6.

Dynamics of the Closed Circuit. As described above, when a salt solution is forced through the membrane gap, a potential difference is established between the electrodes. If these are connected by means of a load resistor (for the spontaneous cycle) or a current power source, as schematically shown in Figure 7, then (electronic) charge will be transferred from one electrode to the other. This provokes a modification of the potential profile, as the slope of the latter close to the carbon wall must be proportional to the surface charge density at each time t (it is a boundary condition of the problem).

Initially, the constant potential inside the electrode (considered as a perfect conductor) is the steady-state membrane potential evaluated as described in previous paragraphs, according to the cationic or anionic nature of the membrane. Once the two electrodes are connected via the external load as in Figure 7, we calculate the amount of charge transferred in each time interval δt assuming that an external current I is forced to go through the circuit. The charge $I\delta t$ is distributed on the 270 μm thick carbon layer, leading to a surface charge density increment $d\sigma(t)$, which can be calculated knowing the specific surface area of carbon (1600 m^2/g) and

the density (385 kg/m^3) of the carbon layer. Because the concentration of ions in the carbon pores can be very high, and in order to avoid overcrowding, finite volume of the ions must be considered. Among the different procedures to do so we have followed those described in refs 28 and 29. An uncharged Stern adjacent to the carbon surface and with thickness δ comparable to the radius of a hydrated counterion is assumed, so that the Poisson−Boltzmann equation in the interfacial region reads:

$$\frac{\partial^2 \Psi(x, t)}{\partial x^2} = \begin{cases} 0 & \text{inside the Stern layer} \\ -\frac{1}{\varepsilon\varepsilon_0} \sum_{j=1}^{N} z_j e n_j(x, t) & \text{outside the Stern layer} \end{cases}$$

$$n_j(x, t) = \frac{n_j^\infty \exp(-z_j e[\Psi(x, t) - E_m]/k_B T)}{1 + \sum_{i=1}^{N} \frac{n_j^\infty}{n_j^{max}} \exp(-z_j e[\Psi(x, t) - E_m]/k_B T)}$$

(11)

where the finite volume of ions has been taken into account by using n_j^{MAX}, the maximum concentration of the corresponding ionic species. Equation 11 can be solved for each time t, subject to the following conditions:

$$\frac{d\Psi}{dx}\bigg|_{\text{pore center}} = 0$$

$$\frac{d\Psi}{dx}\bigg|_{x=0} = -\frac{\sigma}{\varepsilon\varepsilon_0}$$

$$\Psi|_{x=\delta^-} = \Psi|_{x=\delta^+}$$

$$\frac{d\Psi}{dx}\bigg|_{x=\delta^-} = \frac{d\Psi}{dx}\bigg|_{x=\delta^+}$$

(12)

where the accumulated charge density is calculated as $\sigma(t + dt) = \sigma(t) + d\sigma(t)$.

The process continues until the potential difference between the electrodes goes to zero for a spontaneous cycle or when the current source is stopped. As mentioned, it has been demonstrated that if a current source is used to force the potential beyond the zero value by transferring an additional charge, the power density is much higher than in the spontaneous cycle.[12] Note that we assume that there is no transport of ions inside the electrode (ions need not move all the way through the electrode thickness, and it rather suffices that they get closer or further from the interface to build the EDL, depending on the ionic strength).
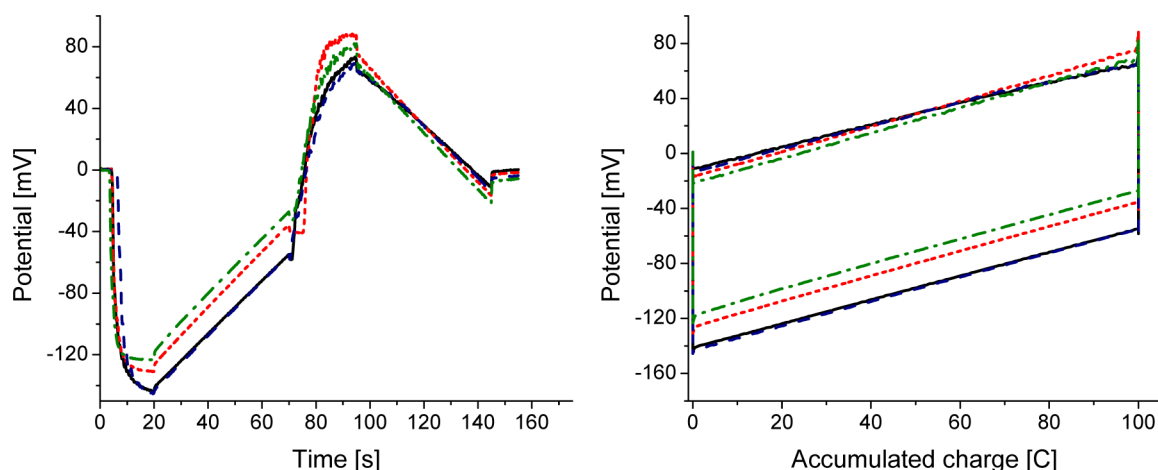
Figure 8. Experimental data of potential-time and potential-charge in CDP cycles, for different combinations of ions as described in Table 4. Black solid lines, NaCl; Blue dashed lines, NaCl + monovalent ions; red dotted lines, real seawater; and green dash-dotted lines, NaCl + divalent ions.
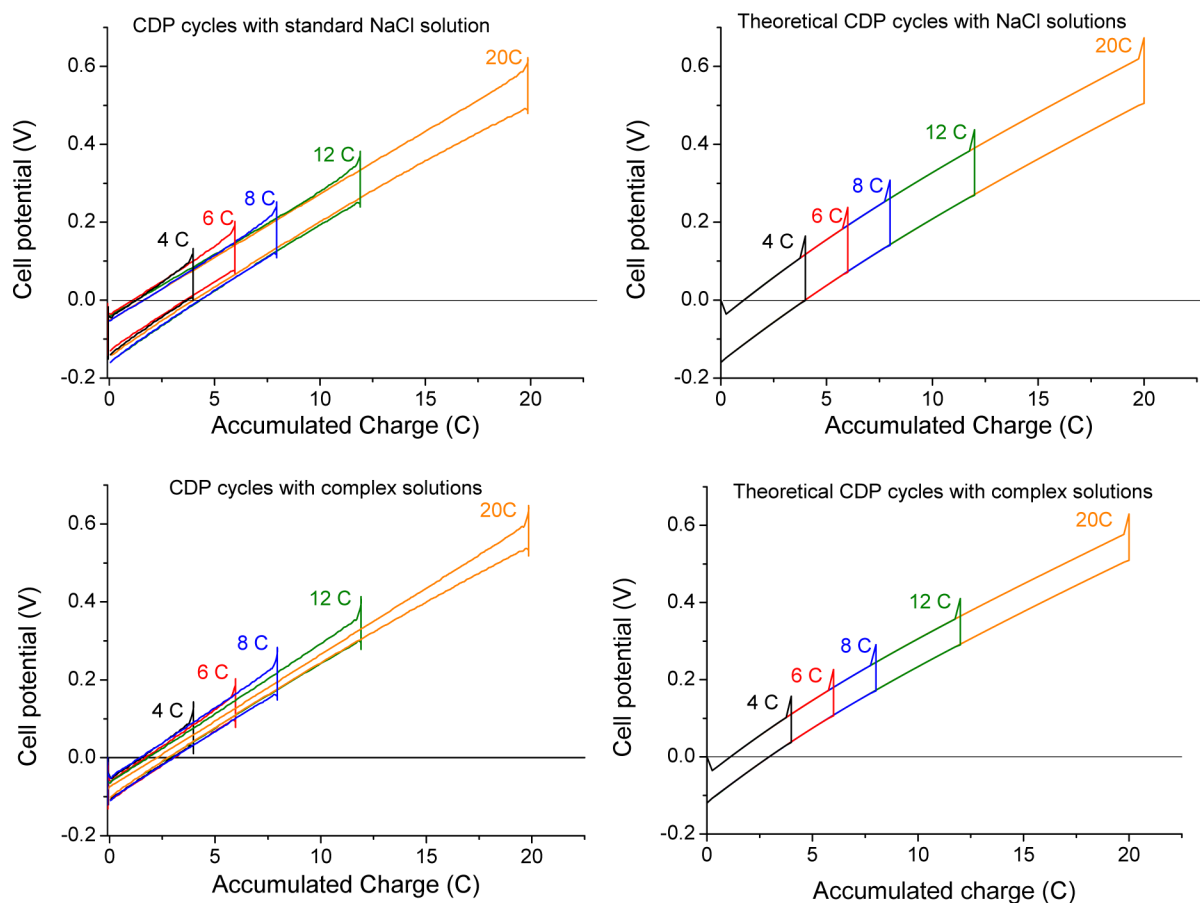
Figure 9. Experimental data (left) and theoretical predictions (right) of CDP cycles for different amounts of externally injected charge, in 511.7 mM concentrated vs 1/30 diluted solutions in (top) pure NaCl and (bottom) artificial seawater (first row in Table 4).

From the set of eqs 11 and 12, we can obtain the potential Ψ for $x = 0$, that is the carbon surface potential, as a function of charge density σ. These data must be compared to the experimental values in closed circuit, as we discuss in the next section.

■ COMPARISON WITH EXPERIMENTS

As mentioned, the ultimate objective of the technique described is the implementation in a coastal site where sea and fresh waters are in close proximity and can be exchanged in the cell. The theoretical predictions concerning the performance of the CDP process indicate that the actual ionic composition of both waters can have a profound effect on the potential reached, particularly when multivalent ions are present. The compositions of the solutions experimentally tested, along with the cell potential and the obtained power density, are given in Table 4.

Figure 8 shows the kinetics of the cycle and the potential-charge relationships experimentally obtained for the ionic

concentrations specified in Table 4. Note, first of all, that the kinetics is roughly the same in KCl and NaCl solutions, confirming that the cell potential is of Donnan origin with no contribution of diffusion potential. The presence of multivalent ions manifests itself in the values reached by the cell potential, and, as a consequence, on the energy and power production, which is reduced by almost 25% in comparison with that reached in pure NaCl solutions.

The modeling of the process was carried out by setting the parameters in such a way that the NaCl results were well reproduced, and modifying them to account for the multi-ionic composition. The agreement between experimental data and predictions is quite satisfactory, as shown in Figure 9, pointing to a coherent description of the CDP method in all kinds of solutions. The procedure used to check the ability of our model to explain the experimental data was as follows:

(i) Assume a simple salt, NaCl, and search, by solving eqs 1−7, for a membrane charge yielding the experimental value of 150 mV for the membrane potential. The charge density found was 9.65×10^7 C/m^3 (1.0 M), assumed identical for the two membranes (except for its sign).

(ii) Using that charge density as data, recalculate the membrane potential in the case of the multi-ionic solutions. With this, we found a Donnan potential of −65 mV for the cationic membrane and −55 mV for the anionic one, that is, a membrane potential of 110 mV, almost identical to the experimental findings.

The procedure involved calculating the charge density at the electrode solution interface. From this, we evaluate the potential profile such that its slope at the interface equals the charge density at each step. In the spontaneous-potential approach, the electrodes reach zero potential and their final surface charge, as shown in Figure 7 for one example case. If the forcing cycle is used, then the circuit remains closed during the time that the external current flows through the cell. The procedure just described allows finding the charge-potential relationships to be compared to the experimental data; this is done in the right panel of Figure 9. Note that the internal resistance of the cell is included in the calculations and explains the spikes observed when the circuit is closed at the end of each cycle. The values used for the internal resistance in both conditions were published by Liu et al.,[12] and they amounted to 0.1 Ω and 0.7 Ω in sea and fresh water, respectively. The effect of electrode geometry on these values has been discussed by Burheim et al.[13]

The agreement is reasonable, considering that no parameters are used, and that the problem is solved on a first-principles basis. Both theory and experiment indicate a measurable reduction of the amount of energy (area enclosed by the cycles) available in the case of multi-ionic solutions. A discrepancy is also clear, and that refers to the fact that we are in reality modeling the capacitance of the double layer, which is not constant, but potential-dependent, so that the relation cannot be linear (as experimentally found), except at high potentials. A way out of this limitation is consideration of the existence of a charged Stern layer, but this appears as an unnecessary complicating aspect of the model, not adding too much to our knowledge of the CDP process.

CONCLUSIONS

In order to understand the role of multivalent ions in solution in the field of energy production by solution exchange, we have analyzed carefully the whole process in a membrane electrode assembly, developed for that purpose. Our study involved both open circuit, when the membrane potential is established, and closed circuit, when a current flow through an external load is produced. The presence of divalent counterions in solution produces a fall in membrane potential, even if their concentration is low. The theoretical model outlined here predicts that some divalent species, Ca^{2+} and Mg^{2+}, are transported against their concentration gradients. This is an important conclusion for future applications, and agrees well with our experimental results. Both theory and experiments show that the presence of multivalent ions reduces the values reached by the cell potential, and, as a consequence, the maximum energy and power production.

AUTHOR INFORMATION

Corresponding Author

*E-mail: sahualli@ugr.es.

Notes

The authors declare no competing financial interest.

REFERENCES

(1) Bijmans, M.; Burnheim, O.; Bryak, M.; Delgado, A. V.; Hack, P.; Mantegazza, F.; Tennison, S.; Hamelers, B. CAPMIX—Deploying Capacitors for Salt Gradient Power Extraction. *Energy Procedia* **2012**, *20*, 108−115.

(2) Brogioli, D. Extracting Renewable Energy from a Salinity Difference Using a Capacitor. *Phys. Rev. Lett.* **2009**, *103* (058501), 1−4.

(3) Rica, R. A.; Ziano, R.; Salerno, D.; Mantegazza, F.; Bazant, M. Z.; Brogioli, D. Electro-diffusion of Ions in Porous Electrodes for Capacitive Extraction of Renewable Energy from Salinity Differences. *Electrochim. Acta* **2013**, *92*, 304−314.

(4) Jimenez, M. L.; Fernandez, M. M.; Ahualli, S.; Iglesias, G.; Delgado, A. V. Predictions of the Maximum Energy Extracted from Salinity Exchange inside Porous Electrodes. *J. Colloid Interface Sci.* **2013**, *402*, 340−349.

(5) Rica, R. A.; Brogioli, D.; Ziano, R.; Salerno, D.; Mantegazza, F. Ions Transport and Adsorption Mechanisms in Porous Electrodes During Capacitive-Mixing Double Layer Expansion (CDLE). *J. Phys. Chem. C* **2012**, *116*, 16934−16938.

(6) Brogioli, D.; Zhao, R.; Biesheuvel, P. M. A Prototype Cell for Extracting Energy from a Water Salinity Difference by Means of Double Layer Expansion in Nanoporous Carbon Electrodes. *Energy Environ. Sci.* **2011**, *4*, 772−777.

(7) Iglesias, G. R.; Fernández, M. M.; Ahualli, S.; Jiménez, M. L.; Kozynchenko, O. P.; Delgado, A. V. Materials Selection for Optimum Energy Production by Double Layer Expansion Methods. *J. Power Sources* **2014**, *261*, 371−377.

(8) Post, J. W.; Hamelers, H. V. M; Buisman, C. J. N. Energy Recovery from Controlled Mixing Salt and Fresh Water with a Reverse Electrodialysis System. *Environ. Sci. Technol.* **2008**, *42*, 5785−5790.

(9) Veerman, J.; Saakes, M.; Metz, S. J.; Harmsen, G. J. Reverse Electrodialysis: Performance of a Stack with 50 Cells on the Mixing of Sea and River Water. *J. Membr. Sci.* **2009**, *327*, 136−144.

(10) Dlugolecki, P.; Gambier, A.; Nijmeijer, K.; Wessling, M. Practical Potential of Reverse Electrodialysis As Process for Sustainable Energy Generation. *Environ. Sci. Technol.* **2009**, *43*, 6888−6894.

15598

dx.doi.org/10.1021/jp504461m | *J. Phys. Chem. C* 2014, 118, 15590−15599

(11) Sales, B. B.; Saakes, M.; Post, J. W.; Buisman, C. J. N.; Biesheuvel, P. M.; Hamelers, H. V. M. Direct Power Production from a Water Salinity Difference in a Membrane-Modified Supercapacitor Flow Cell. *Environ. Sci. Technol.* **2010**, *44*, 5661−5665.

(12) Liu, F.; Schaetzle, O.; Sales, B. B.; Saakes, M.; Buisman, C. J. N.; Hamelers, H. V. M. Effect of Additional Charging and Current Density on the Performance of Capacitive Energy Extraction Based on Donnan Potential. *Energy Environ. Sci.* **2012**, *5*, 8642−8650.

(13) Burheim, O. S.; Liu, F.; Sales, B. B.; Schaetzle, O.; Buisman, C. J. N.; Hamelers, H. V. M. Faster Time Response by the Use of Wire Electrodes in Capacitive Salinity Gradient Energy Systems. *J. Phys. Chem. C* **2012**, *116*, 19203−19210.

(14) Ahualli, S.; Fernández, M. M.; Iglesias, G.; González-Caballero, F.; Delgado, A. V.; Jiménez, M. L. Multi-ionic effects on energy production based on double layer expansion by salinity exchange. *J. Colloid Interface Sci.* **2014**.

(15) Higa, M.; Tanioka, A.; Miyasaka, K. Simulation of theTransport of Ions against Their Concentration Gradient across Charged Membranes. *J. Membr. Sci.* **1988**, *37*, 251−266.

(16) Castilla, J.; GarciaHernandez, M. T.; Moya, A. A.; Hayas, A.; Horno, J. A Study of the Transport of Ions against their Concentration Gradient across Ion-Exchange Membranes Using the Network Method. *J. Membr. Sci.* **1997**, *130*, 183−192.

(17) Vermaas, D. A.; Veerman, J.; Saakes, M.; Nijmeijer, K. Influence of Multivalent Ions on Renewable Energy Generation in Reverse Electrodialysis. *Energy Environ. Sci.* **2014**, *7*, 1434−1445.

(18) Ohshima, H.; Kondo, T. Membrane Potential and Donnan Potential. *Biophys. Chem.* **1988**, *29*, 277−281.

(19) Makino, K.; Ohshima, H.; Kondo, T. Surface-Potential of an Ion-Penetrable Charged Membrane. *J. Theor. Biol.* **1987**, *125*, 367−368.

(20) Goldman, J. C.; McCarthy, J. J. Steady-State Growth and Ammonium Uptake of a Fast-Growing Marine Diatom. *Limnol. Oceanogr.* **1978**, *23*, 695−703.

(21) McLachlan, J. Some Consideration of Growth of Marine Algae in Artificial Media. *Can. J. Microbiol.* **1964**, *10*, 769−782.

(22) Starzak, M. E. *The Physical Chemistry of Membranes*; Academic Press, Inc.: New York, 1984.

(23) Hunter, R. J. *Foundations of Colloid Science, VII*; Oxford Science Publications: Oxford, 1989.

(24) Helfferich, F.; Plesset, M. S. Ion Exchange Kinetics—Nonlinear Diffusion Problem. *J. Chem. Phys.* **1958**, *28*, 418−424.

(25) Schlogl, R.; Helfferich, F. Comment on the Significance of Difussion Potentials in Ion Exchange Kinetics. *J. Chem. Phys.* **1957**, *26*, 5−7.

(26) Conti, F.; Eisenman, G. Non-Steady State Membrane Potential of Ion Exchangers with Fixed Sites. *Biophys. J.* **1965**, *5*, 247−256.

(27) Levich, V. G. *Physicochemical Hydrodynamics*; Prentice Hall: Englewood Cliffs, 1962.

(28) Adamczyk, Z.; Warszynski, P. Role of Electrostatic Interactions in Particle Adsorption. *Adv. Colloid Interface Sci.* **1996**, *63*, 41−149.

(29) Borukhov, I. Charge Renormalization of Cylinders and Spheres: Ion Size Effects. *J. Polym. Sci. Pt. B-Polym. Phys.* **2004**, *42*, 3598−3615.